

*Supplementary Information*

**Facile Water Oxidation by Dinuclear Mixed-Valent Co<sup>III</sup>/Co<sup>II</sup>**

**Complexes: Role of Coordinated Water**

*Atanu Dey,<sup>\*#a</sup> Anku Guha,<sup>#a</sup> Vierandra Kumar,<sup>a</sup> Sumit Bawari,<sup>a</sup> Tharangattu N.Narayanan<sup>\*a</sup>,  
and Vadapalli Chandrasekhar<sup>\*a,b</sup>*

<sup>a</sup>Tata Institute of Fundamental Research Hyderabad, Gopanally, Hyderabad- 500107, India.

<sup>b</sup>Department of Chemistry, Indian Institute of Technology Kanpur, Kanpur-208016, India.

\*Corresponding Authors: [atanu130@gmail.com](mailto:atanu130@gmail.com) (A.D.), [tnn@tifrh.res.in](mailto:tnn@tifrh.res.in) (T.N.N) and [vc@iitk.ac.in](mailto:vc@iitk.ac.in) and [vc@tifrh.res.in](mailto:vc@tifrh.res.in) (V.C.).

# these authors contributed equally.

**Single Crystal X-Ray Crystallography**

Crystal data were collected using a XtaLAB AFC12 (RINC): Kappa single diffractometer equipped with graphite-monochromated molybdenum  $K_{\alpha}$  radiation,  $\lambda = 0.71073$  Å. Data were integrated using CrysAlisPro 1.171.39.29d (Rigaku Oxford Diffraction, 2017) software. Empirical absorption correction was done using spherical harmonics, implemented in SCALE3 ABSPACK scaling algorithm. The structures were solved using the SHELXT structure solution program using Direct Methods and refined with the SHELXL refinement package<sup>1,2</sup> using Least Squares minimization in the Olex-2 software.<sup>3</sup> All the non-hydrogen atoms were refined with anisotropic thermal parameters. All the hydrogen atoms were placed in geometrically calculated

positions or found in the Fourier difference map and included in the refinement process using a riding model. All the mean plane analyses and crystallographic figures have been generated using the DIAMOND software (version 3.2). Crystal data and structure refinement parameters are tabulated in Table S1.

Table S1. Details of the data collection and refinement parameters for complexes **1a** and **3**.

Compound		<b>1a</b>	<b>3</b>
Formula		C <sub>58</sub> H <sub>84</sub> Co <sub>4</sub> N <sub>6</sub> O <sub>31</sub>	C <sub>33</sub> H <sub>47</sub> Co <sub>2</sub> N <sub>2</sub> O <sub>17</sub>
MW /g.mol <sup>-1</sup>		1597.03	861.58
Crystal system		triclinic	Triclinic
Temperature/K		298	120(10)
Space group		<i>P</i> -1	<i>P</i> -1
Unit cell dimensions	<i>a</i> (Å)	8.929(2)	8.863(3)
	<i>b</i> (Å)	10.149(3)	10.178(3)
	<i>c</i> (Å)	19.894(5)	19.785(6)
	$\alpha$ (°)	85.875(2)	99.539(2)
	$\beta$ (°)	89.344(2)	91.887(2)
	$\gamma$ (°)	74.882(2)	92.049(2)
<i>V</i> /Å <sup>3</sup> ; <i>Z</i>		1735.99(8); 1	1757.68(10); 2
$\rho_{\text{calc}}$ /g/cm <sup>3</sup>		1.528	1.628
$\mu$ /mm <sup>-1</sup>		1.030	1.026
<i>F</i> (000)		830	898
Crystal size (mm <sup>3</sup> )		0.25 × 0.2 × 0.12	0.06 × 0.034 × 0.02
$\theta$ range (°)		4.11 to 25.03	4.12 to 25.03
Limiting indices		-10 ≤ <i>h</i> ≤ 10 -12 ≤ <i>k</i> ≤ 12 -23 ≤ <i>l</i> ≤ 20	-10 ≤ <i>h</i> ≤ 10 -11 ≤ <i>k</i> ≤ 12 -23 ≤ <i>l</i> ≤ 23
Reflections collected		30267	34232
Unique reflections [ <i>R</i> <sub>int</sub> ]		6097 [0.1502]	6186 [0.0382]
Data/restraints/parameters		6097/6/452	6186/6/509
GOOF on <i>F</i> <sup>2</sup>		1.058	1.043
Final <i>R</i> indices [ <i>I</i> > 2σ( <i>I</i> )]		<i>R</i> <sub>1</sub> = 0.0642 <i>wR</i> <sub>2</sub> = 0.1841	<i>R</i> <sub>1</sub> = 0.0407 <i>wR</i> <sub>2</sub> = 0.1132
<i>R</i> indices (all data)		<i>R</i> <sub>1</sub> = 0.0715 <i>wR</i> <sub>2</sub> = 0.1910	<i>R</i> <sub>1</sub> = 0.0444 <i>wR</i> <sub>2</sub> = 0.1158
Largest residual peaks (eÅ <sup>-3</sup> )		1.50/-0.63	0.65/-1.11

CCDC Number	2056354	2056355
-------------	---------	---------

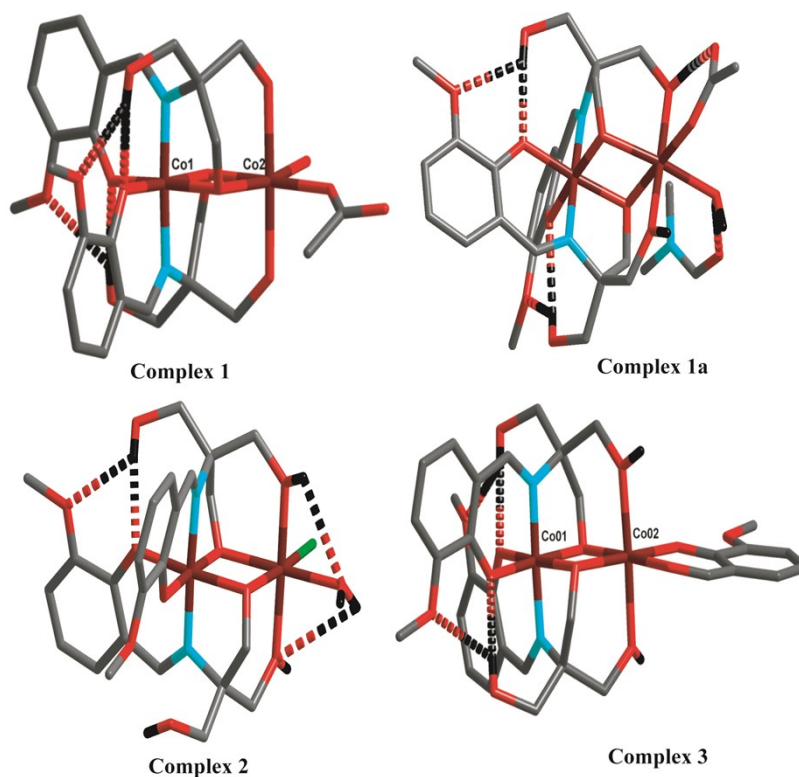


Figure S1. Molecular structure of complexes **1–3** used in this study.

Table S2. Comparison of bond lengths in complexes **1**, **1a** and **3**.

<b>1</b>			<b>1a</b>			<b>3</b>		
Co1	O <sub>phenolate</sub>	1.897(5)	Co1	O <sub>phenolate</sub>	1.907(3)	Co1	O <sub>phenolate</sub>	1.896(2)
Co1	O <sub>phenolate</sub>	1.888(4)	Co1	O <sub>phenolate</sub>	1.880(3)	Co1	O <sub>phenolate</sub>	1.886(2)
Co1	O <sub>CH2O</sub>	1.894(5)	Co1	O <sub>CH2O</sub>	1.899(3)	Co1	O <sub>CH2O</sub>	1.91(2)
Co1	O <sub>CH2O</sub>	1.901(4)	Co1	O <sub>CH2O</sub>	1.904(3)	Co1	O <sub>CH2O</sub>	1.921(2)
Co1	N <sub>imine</sub>	1.888(6)	Co1	N <sub>imine</sub>	1.883(3)	Co1	N <sub>imine</sub>	1.888(2)
Co1	N <sub>imine</sub>	1.892(6)	Co1	N <sub>imine</sub>	1.886(3)	Co1	N <sub>imine</sub>	1.886(2)
Co2	O <sub>CH2O</sub>	2.023(5)	Co2	O <sub>CH2O</sub>	2.019(3)	Co2	O <sub>CH2O</sub>	2.026(2)
Co2	O <sub>CH2O</sub>	2.075(5)	Co2	O <sub>CH2O</sub>	2.045(3)	Co2	O <sub>CH2O</sub>	2.048(2)
Co2	O <sub>OH</sub>	2.153(5)	Co2	O <sub>OH</sub>	2.161(3)	Co2	O <sub>phenolate</sub>	1.990(2)
Co2	O <sub>acetate</sub>	2.023(6)	Co2	O <sub>acetate</sub>	2.062(3)	Co2	O <sub>OH</sub>	2.193(2)
Co2	O <sub>water</sub>	2.108(6)	Co2	O <sub>water</sub>	2.104(3)	Co2	O <sub>CHO</sub>	2.064(2)
Co2	O <sub>OH</sub>	2.180(5)	Co2	O <sub>OH</sub>	2.227(3)	Co2	O <sub>OH</sub>	2.212(2)

Co1	Co2	2.992(9)	Co1	Co2	2.982(7)	Co1	Co2	2.979(5)
-----	-----	----------	-----	-----	----------	-----	-----	----------

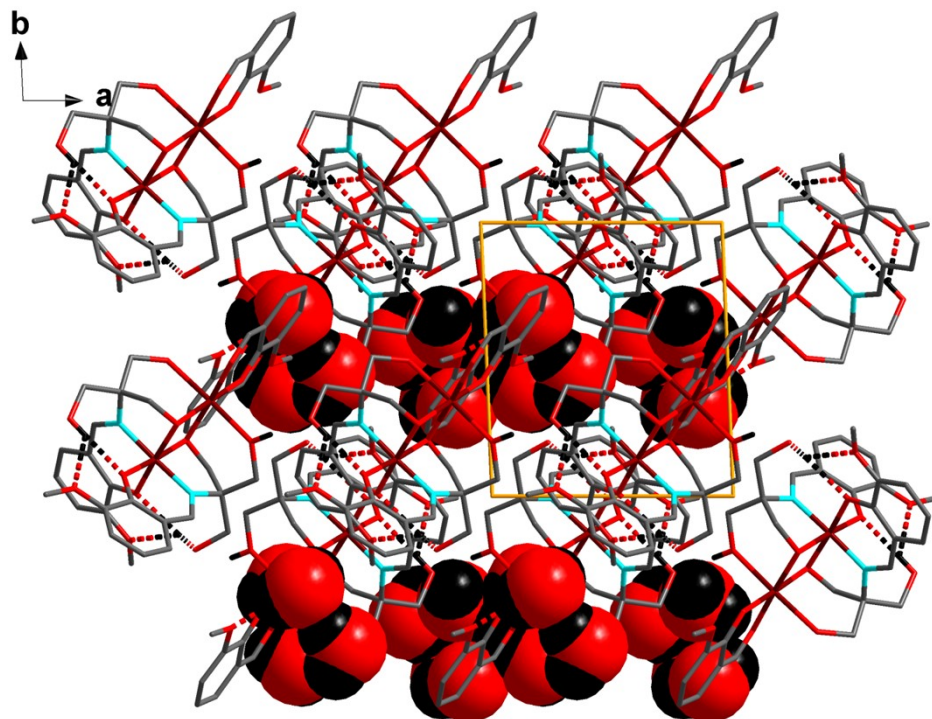


Figure S2. Unit cell packing diagram for complex **3**, water and methanol solvents are shown in space fill model.

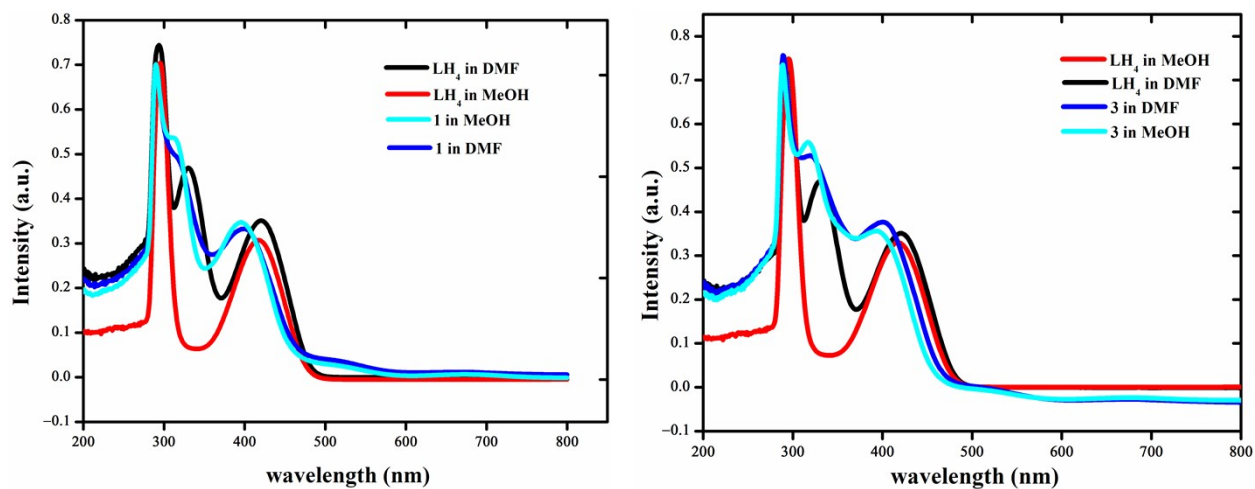
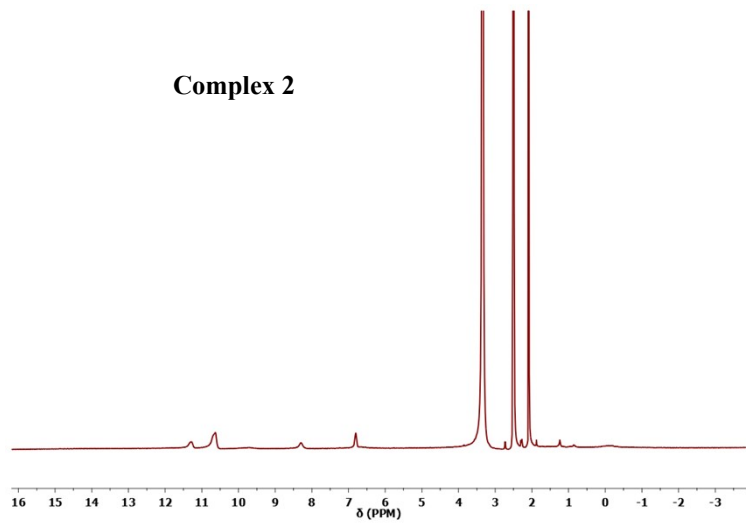
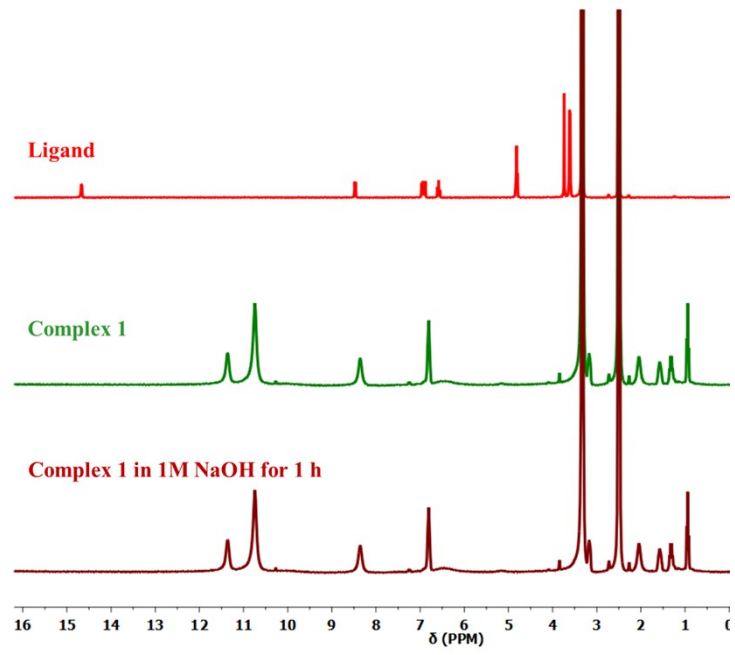


Figure S3. UV/Vis spectra for ligand, complexes **1** (left) and **3** (right) in MeOH and DMF.



Complex 3

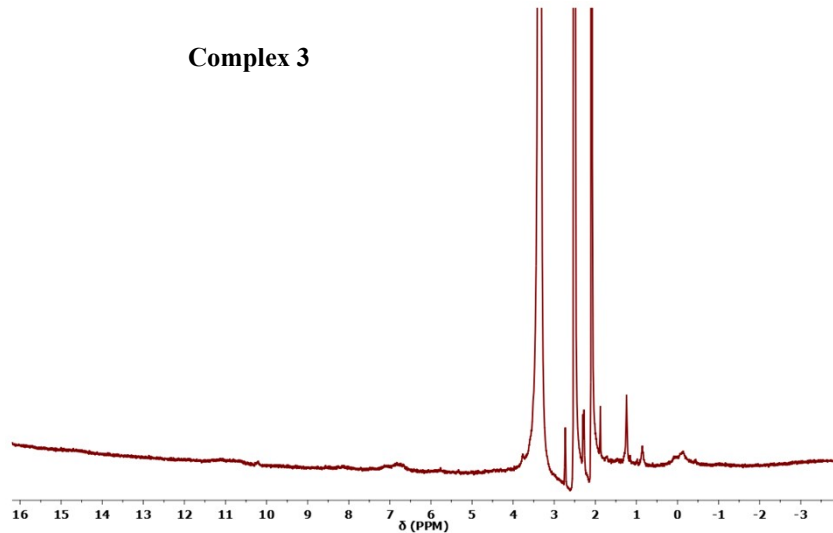


Figure S4. NMR spectra of ligand, complex 1, complex 1 after immersing in 1M NaOH solution for 1 h, complexes 2 and 3. All the NMR spectra are recorded in DMSO-d<sub>6</sub> solvent.

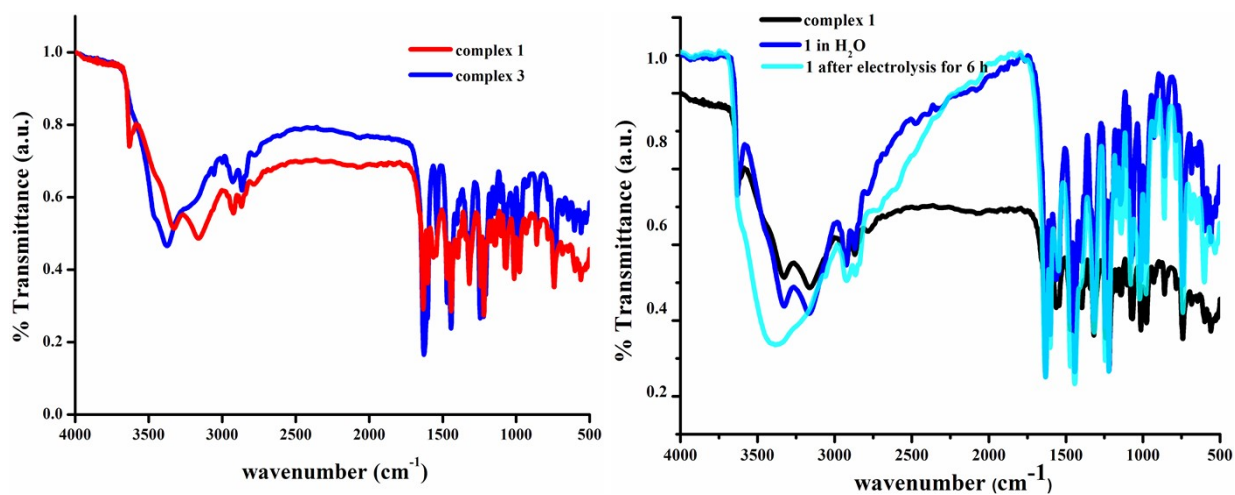


Figure S5. Comparison of the FTIR spectra for complexes 1 and 3 (left), complex 1 and after electrolysis of complex 1 (right).

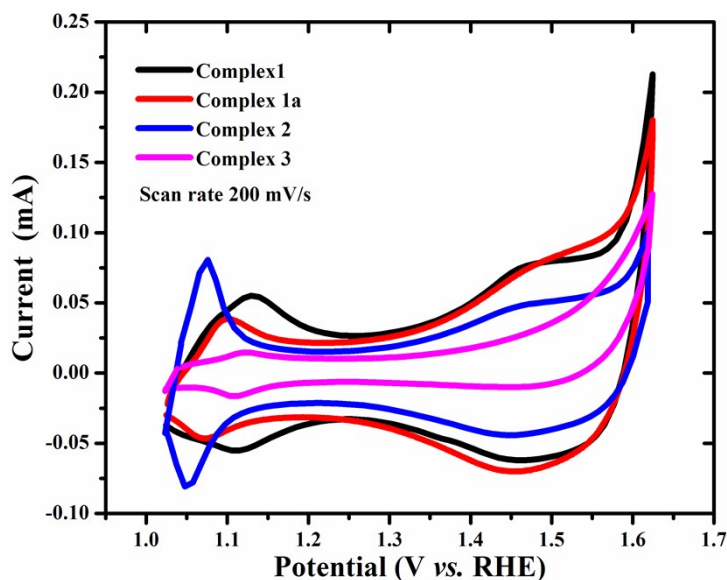


Figure S6. Cyclic voltammograms for complexes **1–3** with scan rate of 200 mV/s.

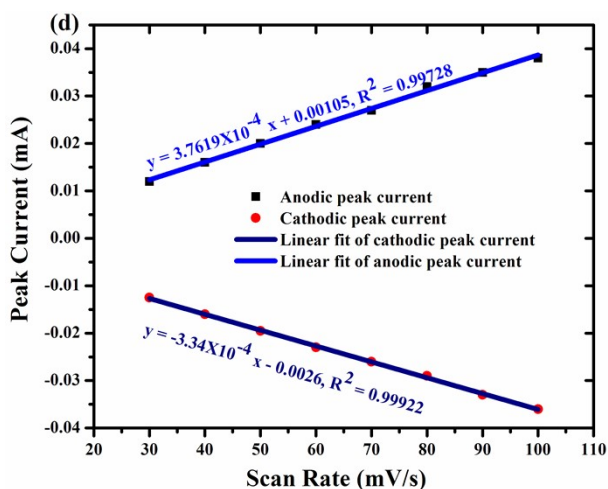
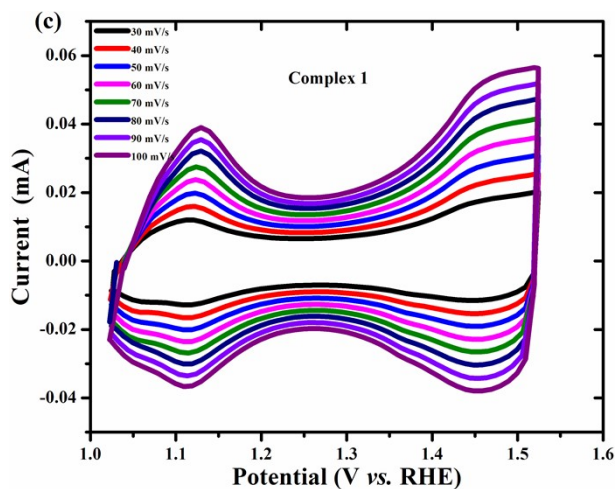
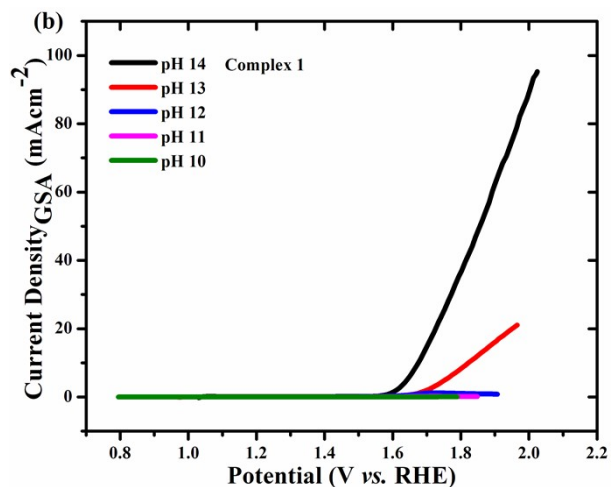
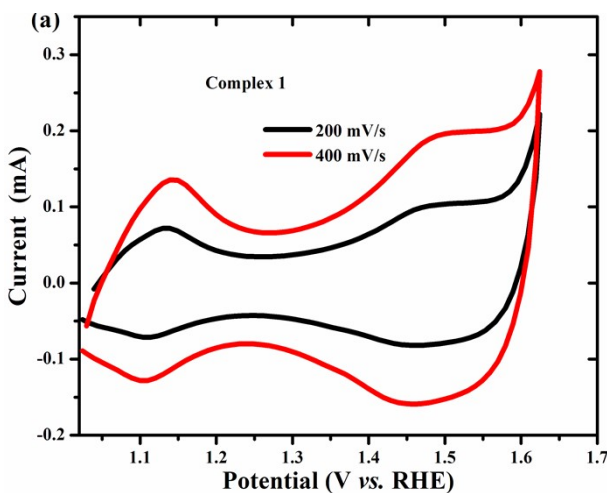
Table S3. Details of the CV and LSV curves for complexes **1–3**, all the potentials are vs RHE.

Complex	Potential (V) for Co <sup>II</sup> to Co <sup>III</sup>	Potential (V) for Co <sup>III</sup> to Co <sup>II</sup>	Potential (V) for Co <sup>IV</sup> =O	Onset potential (V) for WO	Overpotential (mV) for current density 10 mAcm <sup>-2</sup>
<b>1</b>	1.13	1.11	1.49	1.56	445
<b>1a</b>	1.1	1.07	1.48	1.56	445
<b>2</b>	1.07	1.05	1.48	1.58	455
<b>3</b>	1.12	1.11	1.49	1.64	550

Table S4. Details of the EIS analyses for complexes **1–3** at 1.62 V (vs RHE) with varying frequency from 7 MHz to 500 mHz with a sine wave signal of amplitude 10 mV.

Complex	Solution resistance ( $R_s$ ) in $\Omega$	Charge transfer resistance ( $R_{CT}$ ) in $\Omega$
<b>1</b>	55.38	151.1

1a	48.29	154.1
2	55.95	249.7
3	42.35	1040



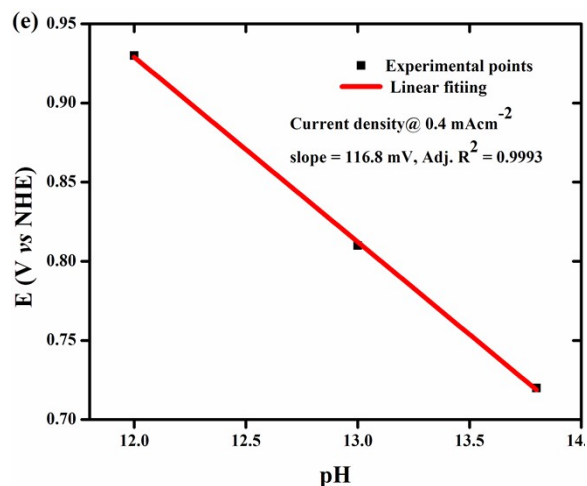
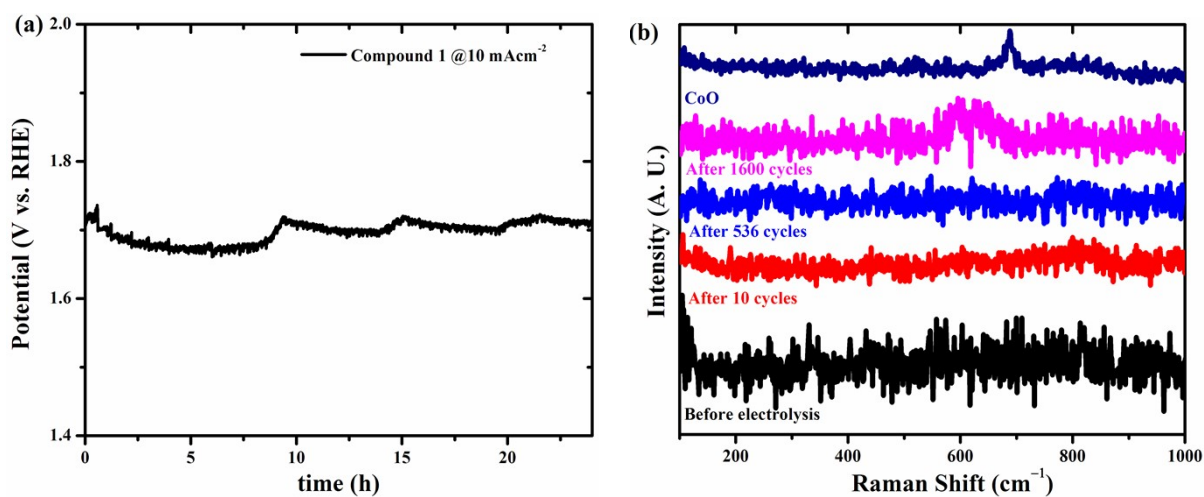


Figure S7. (a) Cyclic voltammograms at different scan rates; (b) LSV curves at different pH, (c) plot of peak current ( $\text{Co}^{\text{II}}$  to  $\text{Co}^{\text{III}}$ ) vs applied potential (RHE) at various scan rates, (d) linear fit of the peak current against scan rates (corresponds to  $\text{Co}^{\text{II}}$  to  $\text{Co}^{\text{III}}$ ) at pH 14 and (e) pH dependency of 116.8 mV/pH corresponds to the involvement of  $1e^- - 2H^+$  in the OER mechanism for complex 1.



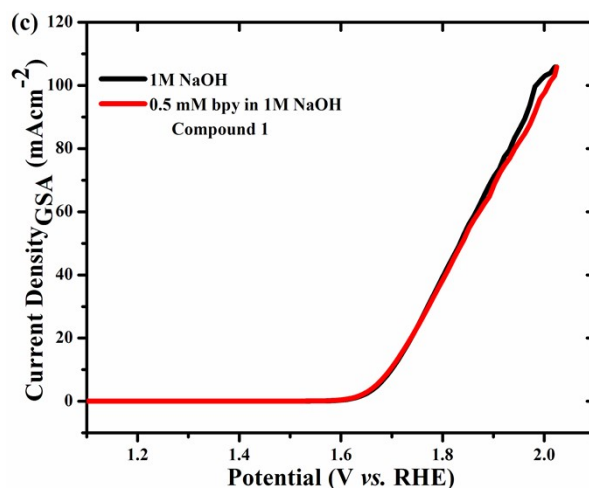
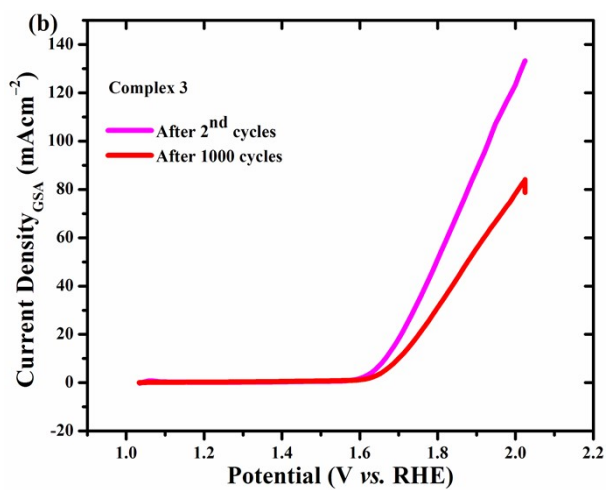
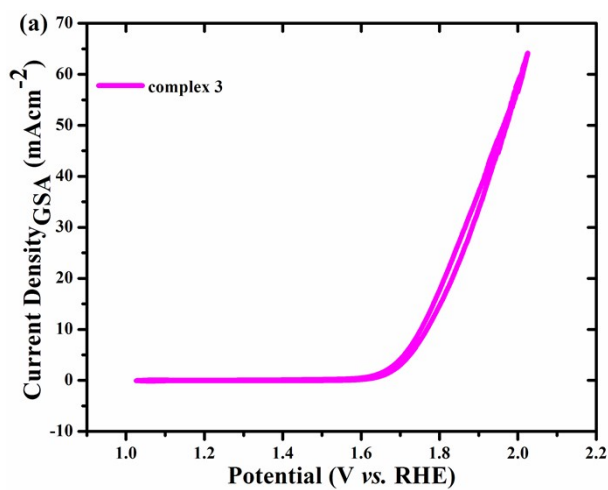


Figure S8. Stability test for the complex **1** during the water oxidation process, (a) chronopotentiometry curve at a constant current density of 10 mAcm<sup>-2</sup>; (b) Raman spectra of the GCE surface (coated with catalyst) after different stages of CV scans and (c) LSV spectra remains unaltered after the addition of bipyridine.



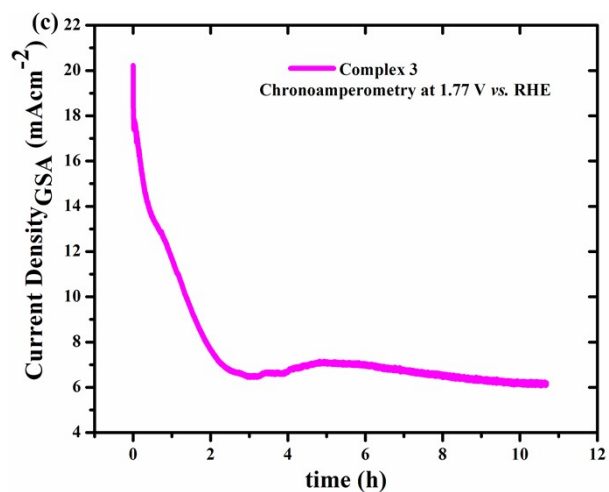


Figure S9. (a) CV, (b) stability test after 1000 cycles CV scans and (c) chronoamperometry for complex 3.

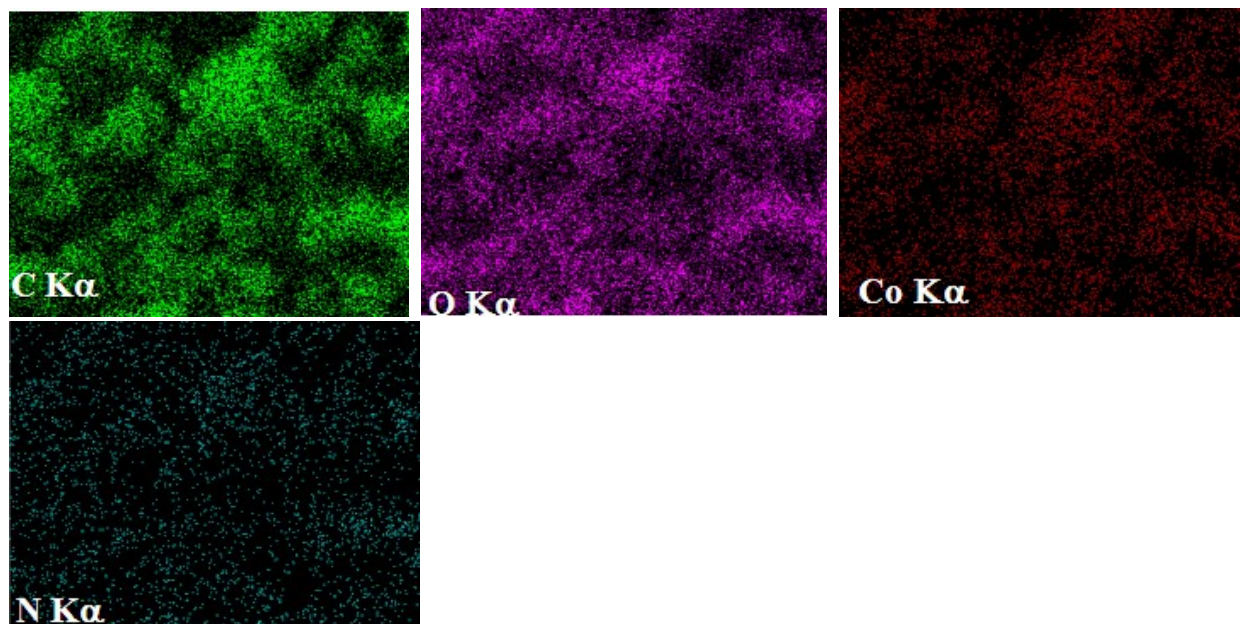
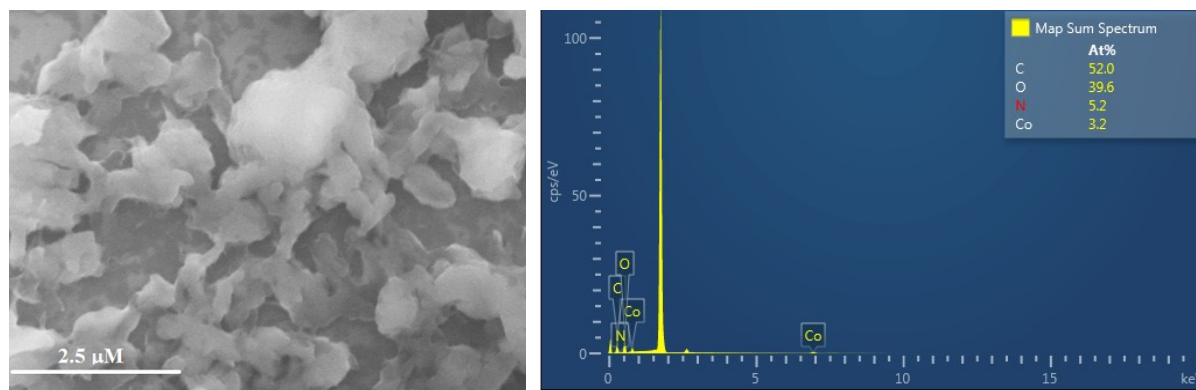


Figure S10. FESEM Image, EDX analysis and elemental mapping for complex 1.

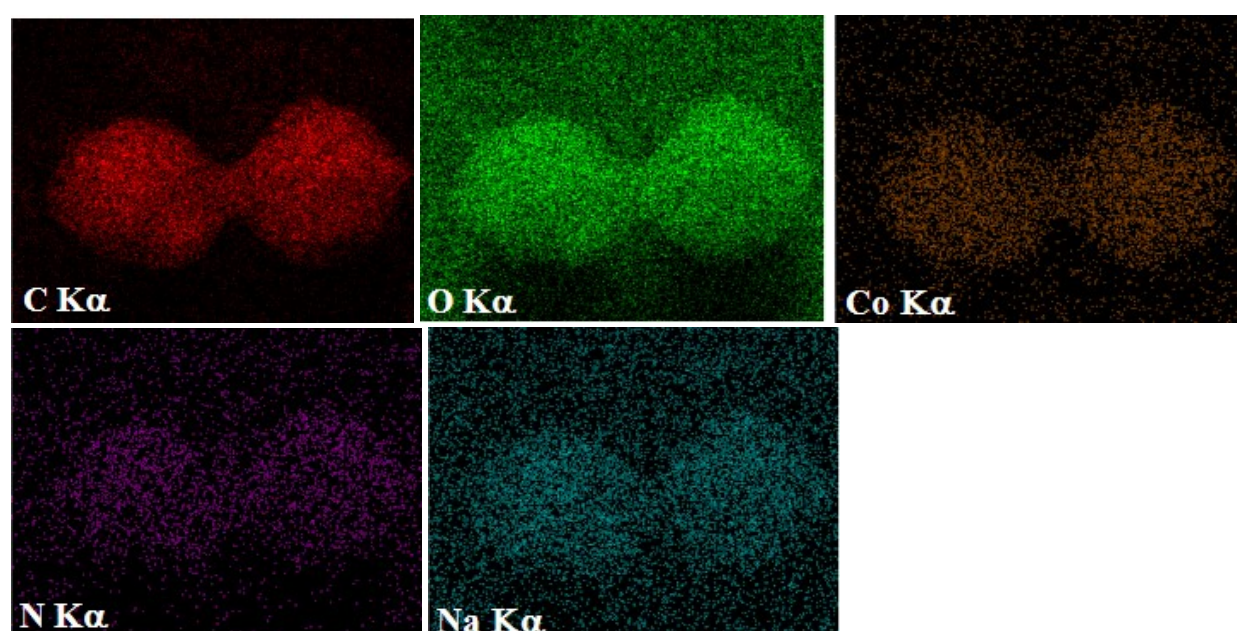
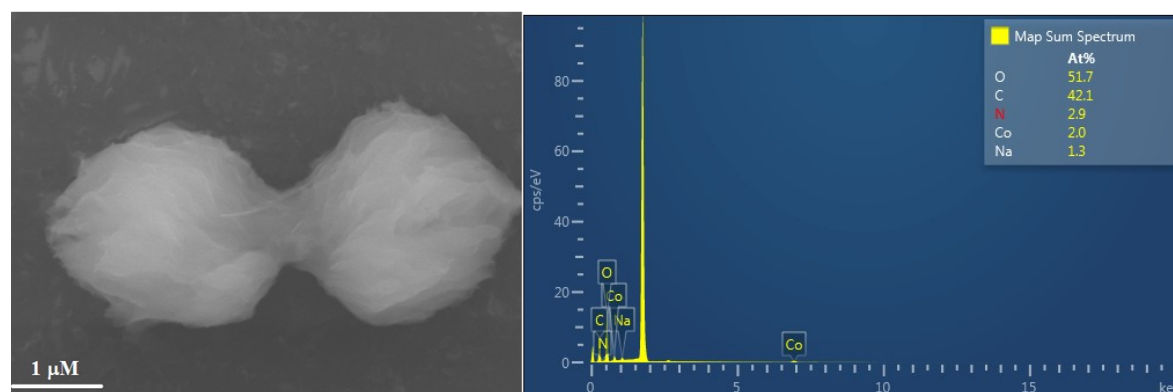
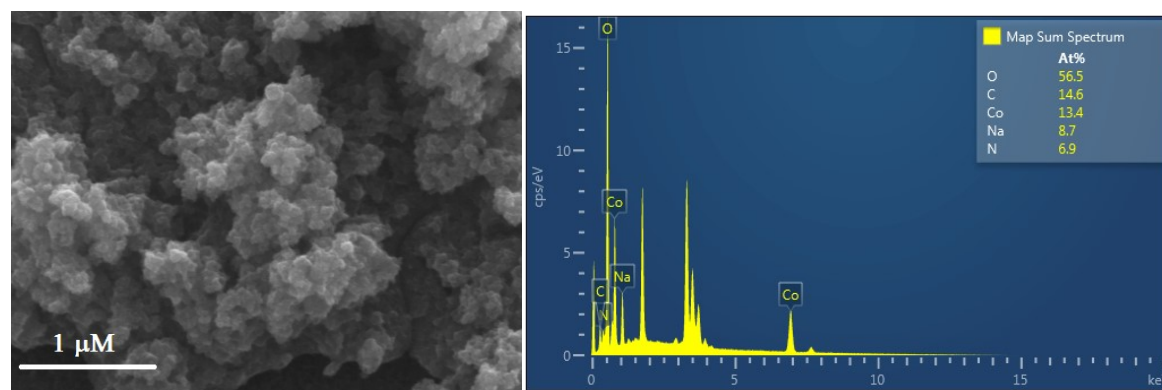


Figure S11. FESEM Image, EDX analysis and elemental mapping for complex 1 after immersing in 1M NaOH solution for 1 h.



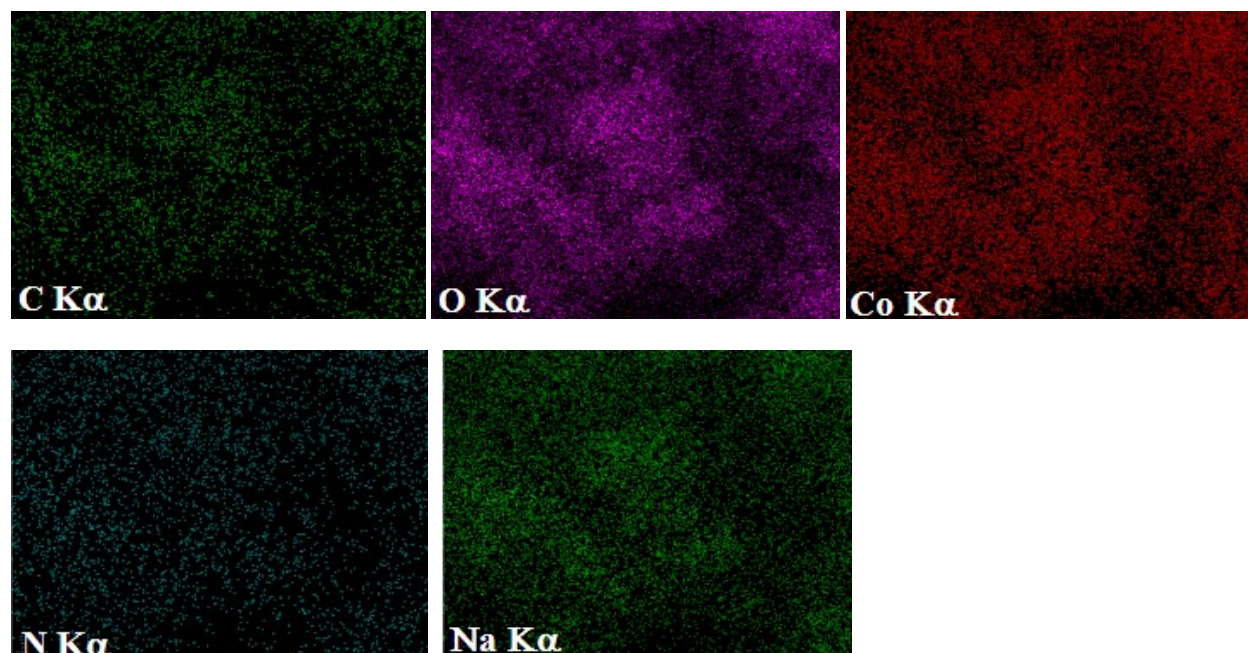


Figure S12. FESEM Image, EDX analysis and elemental mapping for complex **1** after electrolysis for 5 h.

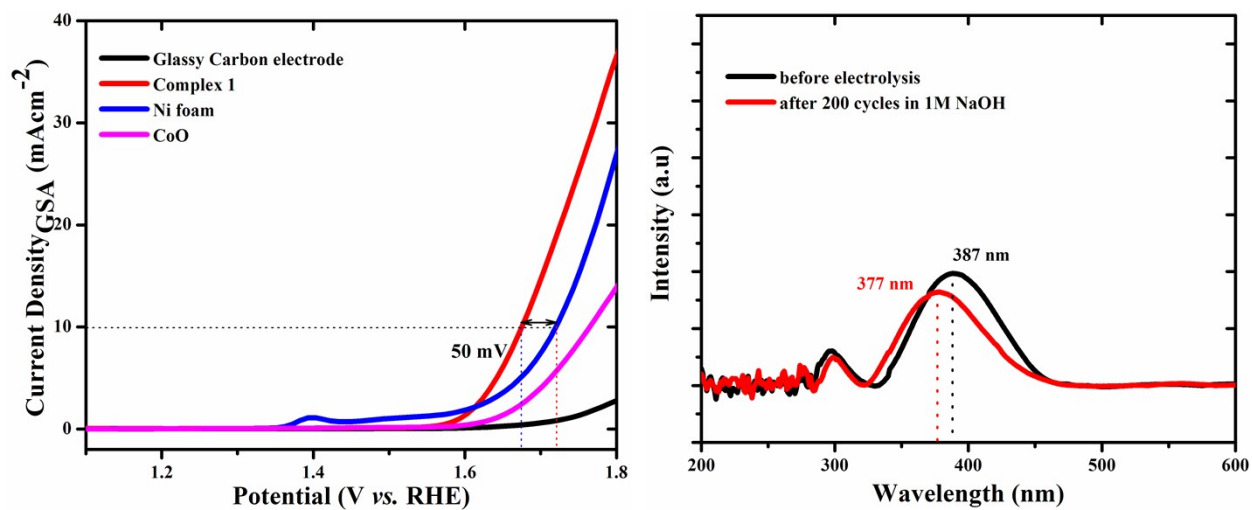


Figure S13. Comparison of LSV curves with commercially available Ni foam,  $\text{CoO}_x$  and complex **1** (left); comparison of electronic absorption before and after electrolysis for complex **1** (right), after electrolysis small blue shift (10 nm) may be due to prolong immersion into 1M NaOH.

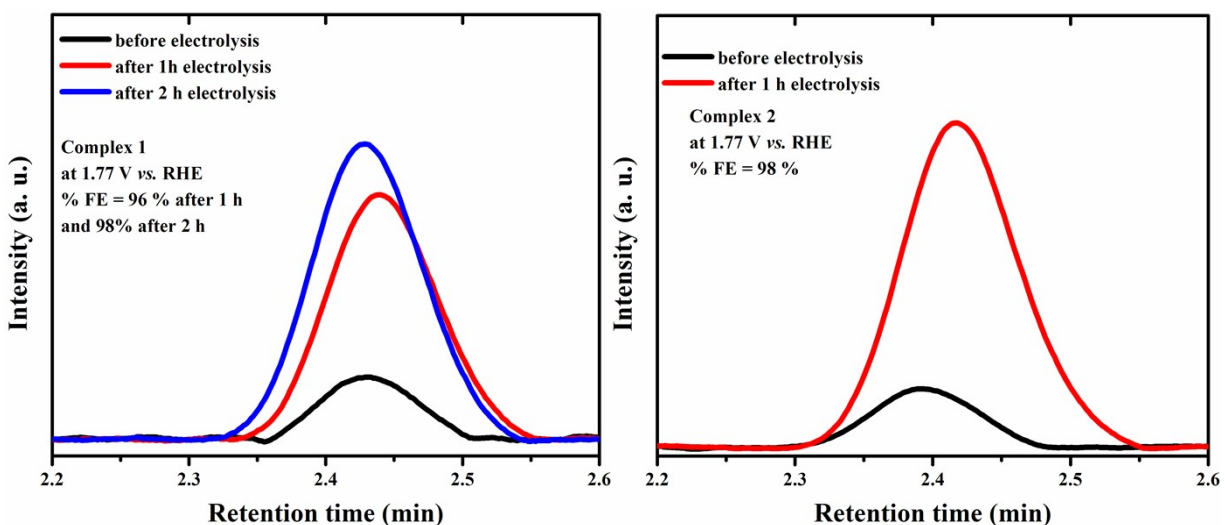


Figure S14. Gas chromatographic measurements data for the quantitative calculation of the evolved O<sub>2</sub> before and after the electrolysis.

### Turn over frequency (TOF) calculation

TOF was calculated according to the literature reported method using equations (1) and (2) J. Am. Chem. Soc. 2011, 133, 14, 5587–5593.

$$\Gamma_0 = \frac{4RT}{An^2F^2} (\text{slope}) \quad \text{-----(1)}$$

$$\text{TOF} = \frac{\text{Current density at } \eta}{4F (\Gamma_0)} \quad \text{-----(2)}$$

$A$  = Electrode surface area (here geometrical surface area);  $R$  = universal gas constant;  $T$  = Temperature;  $n = 1$ , no. of electron transfer during  $\text{Co}^{2+}$  to  $\text{Co}^{3+}$  formation;  $F$  = Faraday constant;  $\eta$  = Overpotential;  $\Gamma_0$  = number of active Co atoms/ $\text{cm}^2$ .

Here, slope =  $3.76 \times 10^{-4} \text{ F}$

$R = 8.314 \text{ J K}^{-1}\text{mol}^{-1}$

$F = 96485 \text{ Coulomb mol}^{-1}$

$A = 0.07 \text{ cm}^2$

$n = 1$

$T = 298 \text{ K}$

Therefore,  $\Gamma_0$  was obtained as  $5.72 \text{ nmol/cm}^2$

With a slope  $3.76 \times 10^{-4}$  (Anodic peak current),  $\Gamma_0$  (number of active Co atoms/cm<sup>2</sup>) is calculated as 5.72 nmol/cm<sup>2</sup>. At 1.59 V (*vs* RHE) with overpotential of 360 mV and current density (1 mAcm<sup>-2</sup>), TOF is calculated as 0.45 s<sup>-1</sup>. At 1.67 V (*vs* RHE) with an overpotential of 440 mV and current density (10 mAcm<sup>-2</sup>), TOF is calculated as 4.5 s<sup>-1</sup>.

Au NP synthesis:

Au nanoparticle (NP) synthesised as per the literature<sup>4</sup>: 100 mL 0.01 wt% HAuCl<sub>4</sub> was heated to boil. Then 0.7 mL sodium citrate 1 wt% was added and refluxed at 140 °C for 1h and cool down to room temperature and then it was directly drop casted over the ‘catalyst’ modified glassy carbon electrode. For the nanoparticle assisted surface enhanced Raman spectra 632 nm laser was used for excitation in a homemade spectrochemical cell.

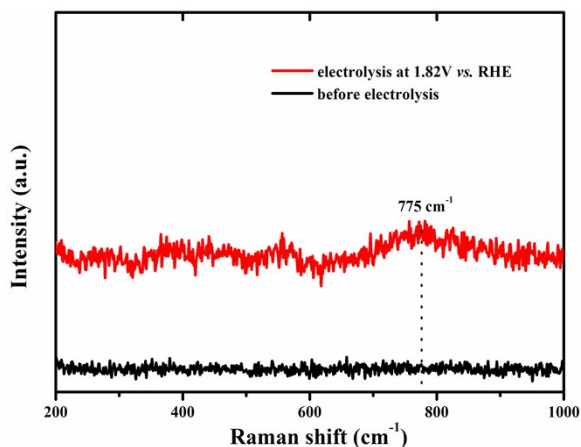


Figure S15. Surface enhanced Raman spectra for complex **1**, where the peak  $\sim 775$  cm<sup>-1</sup> corresponds to Co(IV)=O species.<sup>5</sup>

Table S5. Data summary of Co-based electrocatalysts for oxygen evolution reaction under neutral/basic conditions.

Complexes	Overpotential in mV (current density)#	p <sup>H</sup>	Ref
TPT <sub>2</sub> Co <sup>III</sup>	350	9	<i>Chem. Commun.</i> , 2021, 57, 939.
[Co <sup>II</sup> <sub>8</sub> (OH) <sub>4</sub> (H <sub>2</sub> O) <sub>2</sub> (bdt) <sub>6</sub> ]	352 (2 mA cm <sup>-2</sup> )	7	<i>Chem. Sci.</i> , 2019, <b>10</b> , 9859.
<b>Complex 1</b>	<b>360(1 mA cm<sup>-2</sup>)</b> <b>445(10mA cm<sup>-2</sup>)</b>	<b>14</b>	<b><i>This work</i></b>
<b>Complex 1a</b>	<b>360 (1 mA cm<sup>-2</sup>)</b> <b>445(10mA cm<sup>-2</sup>)</b>	<b>14</b>	
<b>Complex 2</b>	<b>370 (1 mA cm<sup>-2</sup>)</b> <b>455(10mA cm<sup>-2</sup>)</b>	<b>14</b>	
<b>Complex 3</b>	<b>420(1 mA cm<sup>-2</sup>)</b> <b>550(10mA cm<sup>-2</sup>)</b>	<b>14</b>	
[{Co <sup>II</sup> <sub>3</sub> (μ <sub>3</sub> -OH)(BTB) <sub>2</sub> (dpe) <sub>2</sub> } {Co <sup>II</sup> (H <sub>2</sub> O) <sub>4</sub> (DMF) <sub>2</sub> } <sub>0.5</sub> ] <sub>n</sub>	390 (1 mAcm <sup>-2</sup> )	13	<i>Angew. Chem. Int. Ed.</i> 2016, <b>55</b> , 2425.
[Fe <sup>III</sup> <sub>3</sub> (μ <sub>3</sub> O)(bdc) <sub>3</sub> ][Co <sup>II</sup> <sub>2.34</sub> (trz) <sub>3</sub> F <sub>2</sub> (H <sub>2</sub> O) <sub>3.32</sub> (OH) <sub>0.68</sub> ]	439 (10 mA cm <sup>-2</sup> )	13	<i>Chem. Eur. J.</i> 2019, <b>25</b> , 15830 – 15836
[Co <sup>III</sup> (dpaq)(Cl)]	482	8	<i>Dalton Trans.</i> , 2020, 49, 7155.
[Co <sup>II</sup> (Py5)(OH <sub>2</sub> )](ClO <sub>4</sub> ) <sub>2</sub>	500	9.2	<i>Chem. Commun.</i> , 2011, <b>47</b> , 4249.
[Co <sup>II</sup> (tip(Me))(MeCN)][OTf] <sub>2</sub>	500	7	<i>Inorg. Chem.</i> 2019, <b>58</b> , 2, 1391.
[Co <sup>III</sup> (L <sup>N2O3</sup> )H <sub>2</sub> O]	500 (1 mA cm <sup>-2</sup> )	11	<i>Chem. Commun.</i> , 2016, <b>52</b> , 8440
[Fe <sup>III</sup> <sub>3</sub> (μ <sub>3</sub> -O)(bdc) <sub>3</sub> ][Co <sup>II</sup> <sub>2</sub> (trz) <sub>3</sub> Cl <sub>2</sub> (H <sub>2</sub> O) <sub>4</sub> ]	504 (10 mA cm <sup>-2</sup> )	13	<i>Chem. Eur. J.</i> 2019, <b>25</b> , 15830.
[Co <sup>III</sup> (DPKOH) <sub>2</sub> ClO <sub>4</sub>	510	9	<i>Dalton Trans.</i> , 2018, <b>47</b> , 16668.
[L <sub>2</sub> Co <sup>II</sup> (CH <sub>3</sub> OH) <sub>4</sub> ]	520 (0.5 mA cm <sup>-2</sup> )	9	<i>Dalton Trans.</i> , 2017, <b>46</b> , 16321.

$[(\text{TPA})\text{Co}^{\text{III}}(\mu\text{-OH})(\mu\text{-O}_2)\text{Co}^{\text{III}}(\text{TPA})](\text{ClO}_4)_3$	540	8	<i>Angew. Chem. Int. Ed.</i> 2014, <b>53</b> , 14499.
$[\text{Fe}^{\text{III}}_3(\mu_3\text{-O})(\text{bdc})_3][\text{Co}^{\text{II}}_2(\text{trz})_3\text{Br}_2(\text{H}_2\text{O})_4]$	568 (10 mA $\text{cm}^{-2}$ )	13	<i>Chem. Eur. J.</i> 2019, <b>25</b> , 15830.
$[\text{Co}^{\text{III}}(\text{tpfc})]$	580 (1.5 mA $\text{cm}^{-2}$ )	7	<i>Phys. Chem. Chem. Phys.</i> , 2017, <b>19</b> , 9755-9761
$\text{Co}^{\text{II}}\text{-TDMImP}$	583	7	<i>Proc. Natl. Acad. Sci. U.S.A</i> 2013, <b>110</b> , 15579.
$\text{Co}^{\text{III}}\text{H}^{\beta\text{F}}\text{CX-CO}_2\text{H}$	633	7	<i>J. Am. Chem. Soc.</i> 2011, 133, 9178-9180
$\text{Co}^{\text{II}}\text{SO}_4$	660	8.3	<i>Chem. Eur. J.</i> , 2020, <b>26</b> , 711-720
$\text{K}_6[\text{Co}^{\text{II}}\text{W}_{12}\text{O}_{40}]\text{@ZIF8}$	784 (1 mA $\text{cm}^{-2}$ )	7	<i>Angew. Chem. Int. Ed.</i> 2018, <b>57</b> , 1918.
$\text{Co}^{\text{II}}\text{-TTMAP}$	920	7	<i>Proc. Natl. Acad. Sci. U.S.A</i> 2013, <b>110</b> , 15579.

# We have included the current densities those are mentioned in the paper.

## References

1. G. Sheldrick, *Acta Crystallogr., Sect. A*, 2015, **71**, 3-8.
2. G. Sheldrick, *Acta Crystallogr., Sect. C*, 2015, **71**, 3-8.
3. O. V. Dolomanov, L. J. Bourhis, R. J. Gildea, J. A. K. Howard and H. Puschmann, *J. Appl. Crystallogr.*, 2009, **42**, 339-341.
4. C.-Y. Li, J.-B. Le, Y.-H. Wang, S. Chen, Z.-L. Yang, J.-F. Li, J. Cheng and Z.-Q. Tian, *Nat. Mater.*, 2019, **18**, 697-701.

5. B. Wang, Y.-M. Lee, W.-Y. Tcho, S. Tussupbayev, S.-T. Kim, Y. Kim, M. S. Seo, K.-B. Cho, Y. Dede, B. C. Keegan, T. Ogura, S. H. Kim, T. Ohta, M.-H. Baik, K. Ray, J. Shearer and W. Nam, *Nat. Commun.*, 2017, **8**, 14839.